## Pulsar Nulling and Vacuum Radio Emission from Axion Clouds

Andrea Caputo, 1,\* Samuel J. Witte, 2,3,† Alexander A. Philippov, 4 and Ted Jacobson <sup>1</sup>Department of Theoretical Physics, CERN, Esplanade des Particules 1, P.O. Box 1211, Geneva 23, Switzerland <sup>2</sup>Rudolf Peierls Centre for Theoretical Physics, University of Oxford, Parks Road, Oxford OX1 3PU, United Kingdom <sup>3</sup>Departament de Física Quàntica i Astrofísica and Institut de Ciencies del Cosmos (ICCUB), Universitat de Barcelona, Diagonal 647, E-08028 Barcelona, Spain

<sup>4</sup>Department of Physics, University of Maryland, College Park, Maryland 20742, USA

(Received 13 December 2023; revised 4 June 2024; accepted 23 July 2024; published 17 October 2024)

Nonrelativistic axions can be efficiently produced in the polar caps of pulsars, resulting in the formation of a dense cloud of gravitationally bound axions. Here, we investigate the interplay between such an axion cloud and the electrodynamics in the pulsar magnetosphere, focusing specifically on the dynamics in the polar caps, where the impact of the axion cloud is expected to be most pronounced. For sufficiently light axions  $m_a \lesssim 10^{-7}$  eV, we show that the axion cloud can occasionally screen the local electric field responsible for particle acceleration and pair production, inducing a periodic nulling of the pulsar's intrinsic radio emission. At larger axion masses, the small-scale fluctuations in the axion field tend to suppress the backreaction of the axion on the electrodynamics; however, we point out that the incoherent oscillations of the axion in short-lived regions of vacuum near the neutron star surface can produce a narrow radio line, which provides a complementary source of radio emission to the plasma-resonant emission processes identified in previous work. While this Letter focuses on the leading order correction to pair production in the magnetosphere, we speculate that there can exist dramatic deviations in the electrodynamics of these systems when the axion backreaction becomes nonlinear.

DOI: 10.1103/PhysRevLett.133.161001

The QCD axion and axionlike particles are amongst the most compelling candidates for physics beyond the standard model, owing to their ability to resolve major outstanding problems in modern physics (such as the question of why QCD conserves charge-parity symmetry [1–4], and the nature of dark matter [5,6]), and the fact that they arise ubiquitously in well-motivated high-energy theories such as string theory [7–11].

Significant progress has been made in understanding how to search for and detect axions, with a majority of experiments and proposals attempting to observe the coupling of axions to electromagnetism (see, e.g., [12] for a review). One of the particularly promising ideas that has been put forth to indirectly detect axions is to point radio telescopes at neutron stars—the idea being that the large magnetic fields and ambient plasma filling the magnetospheres can dramatically enhance axion-photon interactions. Various observational signatures arising in

Published by the American Physical Society under the terms of the Creative Commons Attribution 4.0 International license. Further distribution of this work must maintain attribution to the author(s) and the published article's title, journal citation, and DOI. Funded by SCOAP<sup>3</sup>.

these systems have been identified [13–38], and preliminary searches have already extended sensitivity to unexplored parameter space [24,25,28].

Recent work in this field has demonstrated that the quasiperiodic vacuum electromagnetic fields in the polar caps of neutron stars can give rise to an enormous injection of axions (i.e., axion field amplitude) with energies (i.e., frequencies)  $\omega_a \sim \mathcal{O}(\text{MHz-GHz})$  [27,28]. Should the axion mass  $m_a$  lie roughly between  $(10^{-9} \text{ eV} \lesssim m_a \lesssim 10^{-4} \text{ eV})$ [39], a sizable fraction of the produced axions will be gravitationally bound to the neutron star [40]. As these are feebly interacting particles, the energy stored in gravitationally bound axions cannot be easily dissipated, and accumulates over the lifetime of the pulsar, generating enormous axion densities [29]. In this Letter, we study the interplay between the growing axion cloud and the electromagnetic fields sourced by the pulsar itself, identifying striking signatures arising from axions in these systems. We focus specifically on the dynamics taking place in the polar caps of pulsars, as they contain large axion field values [29] and pockets of low plasma density that allow for the effect of axion-induced electric fields to be particularly pronounced.

The primary findings of this Letter are twofold. First, we demonstrate that for sufficiently small axion masses, the axion field will induce a periodic screening of the electric field, suppressing particle acceleration and pair production,

Contact author: andrea.caputo@cern.ch

Contact author: samuel.witte@physics.ox.ac.uk

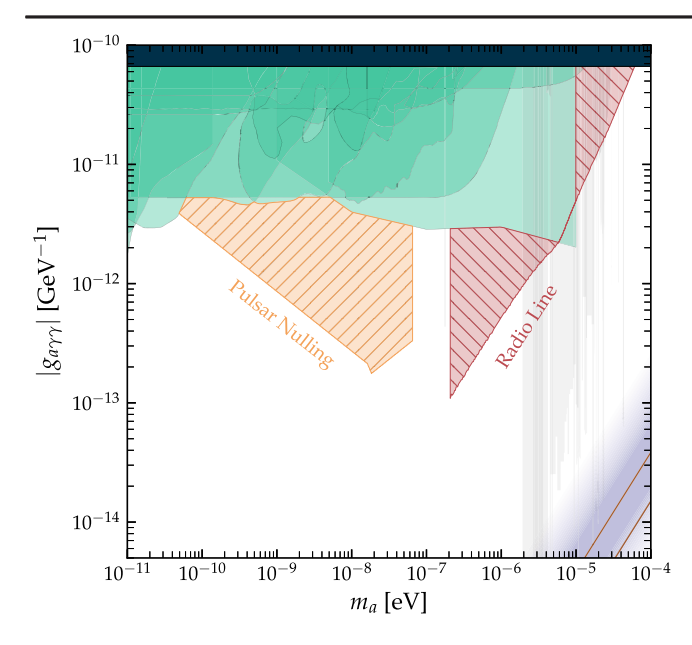


FIG. 1. Parameter space in which bound axions could induce a periodic nulling of (orange), or an observable radio line from (red), the three pulsars studied in this Letter. Shown for reference is the QCD axion band (purple), constraints from indirect astrophysical searches [28,43–54] (teal), CAST [55] (dark blue), axion haloscopes [56–73] (grey; assumes axions are dark matter), and radio line searches in neutron stars [20,25] (grey; assumes axions are dark matter).

and leading to a quasiperiodic cancellation of radio pulses. For heavier axions, the small-scale fluctuations of the axion field drive the axion-induced voltage drop across the polar cap to zero, washing out the impact of the axion. Nevertheless, in this mass range we show that during the so-called "open phase," i.e., a short-lived phase that precedes the onset of pair production, axions can produce a spectral line with  $\mathcal{O}(5)$ %-level width (set by the axion velocity dispersion) that may be observable using existing radio telescopes; owing to the variation in neutron star mass/radius ratios [41,42], there should also exist frequency variations at the  $\mathcal{O}(20)\%$  level across the neutron star population due to gravitational redshifting. We use three known pulsars to illustrate the potential sensitivity of such probes, showing that future observations may be able to significantly improve sensitivity to axions over a wide range of parameter space (see Fig. 1).

Polar cap dynamics in the presence of axions—The generalization of Gauss's and Ampere's laws in the presence of axions is given by [74]

$$\nabla \cdot \vec{E} = \rho - g_{a\gamma\gamma} \vec{B} \cdot \nabla a, \tag{1}$$

$$\nabla \times \vec{B} - \dot{\vec{E}} = \vec{J} + g_{ayy} \dot{a} \, \vec{B} + g_{ayy} \nabla a \times \vec{E}, \tag{2}$$

which suggests the axion field a produces effective charge and current densities  $\rho_a = -g_{a\gamma\gamma}\vec{B}\cdot\nabla a$  and

 $\vec{J}_a = g_{a\gamma\gamma}\dot{a}\,\vec{B} + g_{a\gamma\gamma}\nabla a \times \vec{E}$ . In most contexts, the corrections from the axion are sufficiently small to only perturbatively alter the electrodynamics; we show below, however, that this is not necessarily true in the polar caps of pulsars.

Let us start with an overview of the conventional picture of electrodynamics in the polar caps (see, e.g., [75–77] for further details). In the absence of a dense ambient plasma, the large-scale magnetic field together with the rotating, conducting, neutron star will induce a large electric field; the force exerted by the component of this electric field oriented along the magnetic field,  $E_{\parallel}$ , can greatly exceed that of gravity, and can serve to directly extract charges from the stellar atmosphere. Along open magnetic field lines, this process drives an out-flowing current which serves to sustain the large-scale twist of the magnetic field,  $j_m \equiv \nabla \times B$ . When the current is super-Goldreich-Julian (GJ),  $j_m > \rho_{\rm GJ}$ , where  $\rho_{\rm GJ} = -2\vec{\Omega} \cdot \vec{B}$  (with  $\vec{\Omega}$  and  $\vec{B}$  being the angular velocity and magnetic field of the pulsar), the system develops a large voltage drop, accelerating electrons, which in turn generate high-energy curvature photons that initiate  $e^{\pm}$  production. The resulting dense plasma dynamically screens the electric field via a nonlinear quasiperiodic process that has been shown to source coherent radio emission (see, e.g., [78]). If instead the supplied current is sub-GJ (i.e.,  $j < \rho_{\rm GJ}$ ), the extracted charges screen the field, and the system instead tends toward a steady state in which acceleration, pair production, and coherent radio emission are suppressed.

The stark difference in behavior observed between super- and sub-GJ current densities can be illustrated using a simplified one-dimensional evolutionary model [77]. This toy model is expected to be a reasonable approximation to the initial behavior of the open phase of the gap (particularly for young, active, pulsars). Here, we generalize this to include the impact of an axion background, showing that axion charge densities  $\rho_a \gtrsim \mathcal{O}(10\%) \times \rho_{\mathrm{GJ}}$  can profoundly alter the dynamics of these systems. The one-dimensional model follows the acceleration of the primary particles, which to a very good approximation propagate along the magnetic field lines. The electromagnetic field is assumed to be that of a global force-free magnetosphere with a constant charge density  $\rho_{\rm GJ}$  and current density  $\alpha \rho_{\rm GJ}$ , determined by the (rotating) boundary conditions, plus an additional electric field parallel to the magnetic field and corresponding charge density which are present because the supply of charge from the neutron star atmosphere does not match that of the force-free configuration. Using (1), (2), and the Lorentz force law, and assuming a single sign for the charge (a good approximation when starting with a vacuum field at the polar cap), one can solve for the charge density and velocity [or Lorentz factor  $\gamma(s)$ ] and the electric field component  $E_s$  as functions of distance s along the field lines, with the boundary conditions  $\gamma(0) = 1$ ,  $\gamma_s(0) =$ 0 at the surface of the star, s = 0. This yields

$$\frac{1}{2}\gamma_{,s}^2 = \left(1 - \frac{\rho_a}{\rho_{\rm GJ}}\right)(1 - \gamma) + \left(\alpha - \frac{j_a}{\rho_{\rm GJ}}\right)\sqrt{\gamma^2 - 1},\quad(3)$$

with s in units of the Debye length scale,  $\lambda_D = 1/\omega_{p,GJ}$ .

The ratio  $\alpha \equiv j_m/\rho_{\rm GJ}$  is called the discharge parameter, since it governs the screening of the electric field. We show in Fig. 2 the evolution of the electron Lorentz factor without axions (black) for  $\alpha = 0.9$  (top panel) and  $\alpha = 1.1$  (bottom panel). For  $\alpha > 1$ , the energy continues to increase as the primary particles move away from the surface. As these particles are accelerated they emit curvature radiation along the field line; when the primary particles reach boost factors of  $\gamma \sim 10^6 - 10^8$ , the gamma rays begin pair producing in the background magnetic field, and the production of these pairs leads to a screening of the ambient electric field [75,79–81]. The evolution of the dynamical screening phase is highly nonlinear, and understanding how axions affect this screening (and the subsequent generation of coherent radio emission) requires dedicated simulations; nevertheless, for the purposes of this Letter it is sufficient to focus on pair production as being a necessary step in this process. For  $\alpha < 1$  [82], on the other hand, the evolution of the primary current density is dramatically different. Here, the primary particles immediately begin screening the electric field; consequently, these particles never reach large Lorentz factors, and pair production never occurs. In general,  $\alpha$  is a spatially varying function over the footprints of the open field lines, typically taking on  $\alpha \sim \mathcal{O}(1)$ values, and with the characteristic variance on the order of  $\mathcal{O}(10\%)$  [83,84].

The impact of axions on the evolution of the primary particles is shown in Fig. 2. We assume the axion charge and current densities are oscillatory functions (as expected for classical fields) which are constant over the time and length scales corresponding to the evolution in Fig. 2, and we set  $j_a = 3\rho_a \sim (\omega/k)\rho_a$ , which is a natural value of axions gravitationally bound to the neutron star-see the section Axion production in polar caps and pulsar nulling. The shaded regions encompass the maximal and minimal  $\gamma$ at each point along the trajectory, for values of  $\rho_a$  falling between the indicated limits. For sufficiently large  $\rho_a$ , the presence of the dense axion field induces transitions between the qualitatively different regimes [85]. When the axion coherently suppresses particle acceleration along not just one, but a sufficiently large bundle, of open magnetic field lines, one expects a coincident suppression of coherent radio emission—this is a novel signature which could provide striking evidence of axions in these systems [86].

Thus far we have shown that the behavior of pair production can be dramatically altered by an axion field with  $\rho_a \gtrsim 0.1 \times \rho_{\rm GJ}$ —in the following section we demonstrate that such field values can naturally be reached in many systems. Note that we do not address the impact of axions on the nonlinear dynamical screening phase.

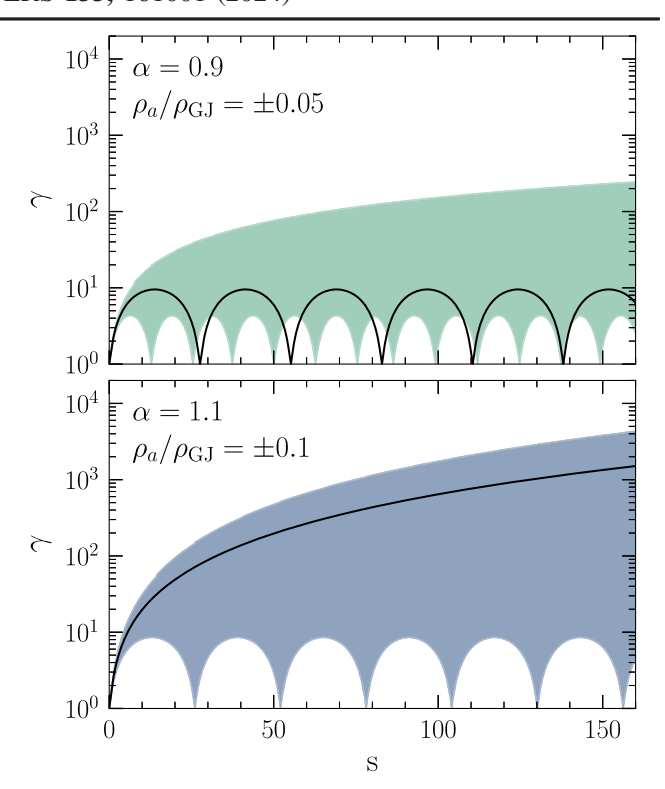


FIG. 2. The evolution of the primary electron beam Lorentz factor [i.e., the solution to Eq. (3)] as a function of distance s from the neutron star surface (in units of  $\lambda_D$ ) for different initial discharge parameters  $\alpha$ . The standard case without axions is shown in black for  $\alpha=0.9$  (top) and 1.1 (bottom), and the effect of perturbing the system with a constant axion charge density  $\rho_a$  is highlighted in the colored bands.

Instead, we focus on the fact that coherent radio emission requires pair production, which in turn requires highenergy particles. Future work will develop simulations of axion electrodynamics extending to the nonlinear phase.

Axion production in polar caps and pulsar nulling—We now turn our attention to the question of how, and when, large axion field values near the surfaces of neutron stars are expected to arise.

It has recently been shown that oscillations induced by the dynamical screening of the electric field in the polar cap source axions with characteristic energies  $\omega_a \lesssim 10^{-4} \text{ eV}$ (this is a consequence of the fact that  $g_{a\gamma\gamma}\vec{E}\cdot\vec{B}$  enters as a source term in the axion's equation of motion). If the axion mass lies in the range  $10^{-10} \lesssim m_a \lesssim 10^{-4} \text{ eV}$ , a sizable fraction of the produced axions will be, at most, semirelativistic, and will remain gravitationally bound to the star itself. Furthermore, since axions interact feebly with the ambient matter they naturally accumulate on long, astrophysical, timescales. For axions in this mass range one thus concludes that pulsars are generically surrounded by dense clouds of axions. That said, is the density of these clouds high enough to impact the electrodynamics as described in the previous section? The answer will be affirmative provided axion production is large and energy dissipation (extracting energy from the cloud) remains small. For simplicity we focus here on the case of light axions (with  $\lambda_a \gtrsim h_{\rm gap}$ ), showing that both conditions can be satisfied for a wide range of parameter space. In the Supplemental Material (SM) [87] we derive similar conclusions for the case of heavy axions ( $\lambda_a \lesssim h_{\rm gap}$ ).

The production of axions in polar caps has been studied using both a semianalytic model and a kinetic plasma simulation [28]. Here, we use the result of [28] to derive analytic estimates of the energy injection rate and the axion density in the polar caps.

The rate at which axions extract energy from the electromagnetic fields is approximately given by [27,28]

$$\frac{dE_{\rm inj}}{dt} \sim \zeta^2 \frac{g_{a\gamma\gamma}^2 m_a^3}{81 \times \tau} r_{\rm pc}^4 h_{\rm gap}^4 B_0^4 \Omega^2, \tag{4}$$

where  $r_{\rm pc} \simeq R_{\rm NS} \sqrt{R_{\rm NS} \Omega}$  is the polar cap radius,  $R_{\rm NS}$  is the radius of the neutron star,  $\Omega$  its rotational frequency,  $B_0$  the surface magnetic field strength,  $\tau \sim 10 h_{\rm gap}$  is the gap periodicity, and

$$h_{\rm gap} \sim 12 \text{ m} \left(\frac{R_c}{10^7 \text{ cm}}\right)^{2/7} \tilde{\Omega}^{-3/7} \tilde{B}_0^{-4/7}$$
 (5)

is the gap height. In Eq. (5), we have introduced the characteristic radius of curvature of open field lines  $R_c \simeq 9 \times 10^7 \ {\rm cm} \sqrt{P/(1\ {\rm sec})}$  [81,88], with  $P=2\pi/\Omega$ , and used the  $\tilde{X}$  notation to denote quantities X which are normalized with respect to those of the Crab pulsar [89,90] (e.g.,  $\tilde{\Omega} \equiv \Omega/\Omega_{\rm crab}$ ). Finally, we have also introduced an order-one fudge factor  $\zeta$ , characterizing the size of  $E_{||}$  with respect to the maximal value  $E_{\rm max} \sim \rho_{GJ} \times h_{\rm gap}$ , with  $\rho_{\rm GJ} \sim -2\vec{B}\cdot\vec{\Omega}$  being the Goldreich-Julian (GJ) charge density (i.e.,  $E_{||} \equiv \zeta E_{\rm max}$ ) [75,91].

Assuming the cloud grows linearly on long timescales (compared to the variability of  $\vec{E} \cdot \vec{B}$ ), the axion energy density at the surface of the neutron star after a time t is roughly given by

$$\epsilon_0(t) \sim \! \frac{3t}{16\pi r_{\rm NS}^3} \frac{dE_{\rm inj}}{dt} \! \sim \! 5 \times 10^{23} \; \frac{{\rm GeV}}{{\rm cm}^3} g_{-12}^2 m_{-8}^3 \tilde{t}_{\rm age} (\tilde{B}_0 \tilde{\Omega})^{8/7},$$

(6)

where  $g_X = g_{a\gamma\gamma}/10^X~{\rm GeV}^{-1}$  and  $m_X = m_a/10^X~{\rm eV}$ , and the exponent 8/7 comes from the implicit dependence on  $B_0$  and  $\Omega$  entering  $h_{\rm gap}$  and  $r_{\rm pc}$ . We can now determine whether sufficiently large axion densities are achievable in these systems by comparing Eq. (6) with the backreaction density, defined as the energy density for which  $\rho_a = \xi \rho_{\rm GJ}$  [with  $\xi \sim \mathcal{O}(1)$  an order-one prefactor]. Given an axion field energy density  $\frac{1}{2}m_a^2a^2$  and the axionic charge density  $\rho_a \sim g_{a\gamma\gamma}Bk_aa$  [Eq. (1)], we have

$$\epsilon_{\rm br} \sim \xi^2 \frac{2\Omega^2 m_a^2}{g_{a\gamma\gamma}^2 k_a^2} \sim 5 \times 10^{20} \ \frac{{\rm GeV}}{{\rm cm}^3} \tilde{\Omega}^2 \bigg( \frac{1}{g_{-12}} \frac{\xi}{0.1} \bigg)^2. \ \ (7)$$

Comparing this with Eq. (6), we see that backreaction densities are achievable in many systems provided  $g_{-12} \gtrsim \mathcal{O}(0.1)$ .

Next, one must determine whether there exists an energy dissipation mechanism that could quench the growth of the cloud before reaching  $\epsilon_{\rm br}$ . For light axions, on-shell photon production is kinematically blocked by the presence of the plasma, and thus all energy dissipated from the axion field must proceed indirectly through the local current—that is to say, the axion-induced electric field helps to accelerate local charges, which in turn dissipate energy via radiation [92]. The net (time-averaged) energy loss can be obtained by computing  $\langle \vec{j} \cdot \vec{E}_a \rangle$ , where  $E_a$  is the axion-induced electric field and  $j_e$  the current. In the SM [93] we show that the leading-order contribution to the axion-induced electric field is given by

$$\vec{E}_a \sim g_{a\gamma\gamma} \frac{\sqrt{2\epsilon_a}}{m_a} \vec{B} e^{-im_a t} \times \mathcal{F}(m_a, h_{\text{gap}}, \omega_p),$$
 (8)

where the factor  $\mathcal{F}$  captures the in-medium suppression. with a uniform vacuum yielding  $\mathcal{F} = 1$ , and a dense uniform plasma yielding  $\mathcal{F} \sim (m_a/\omega_{p,\rm eff})^2 \ll 1$  (where  $\omega_{p,\text{eff}} \equiv \langle \omega_p^2/\gamma^3 \rangle^{1/2}$ , with  $\langle \rangle$  denoting the average over the distribution functions and the species present in the plasma, and the plasma frequency of a single species s defined as  $\omega_{p,s}^2 \equiv q_s^2 n_s / m_s$ , with  $q_s$ ,  $n_s$ , and  $m_s$  the charge, number density, and mass [98]) (with nonuniform geometries, as is relevant for this case, one obtains a suppression interpolating between these limiting regimes, see SM). One can see from Eq. (8) that the electric field is heavily suppressed once plasma is produced, and thus the energy dissipation will be most efficient during the open phase of the gap. Equating the axion production and dissipation rates, one can estimate the maximal axion energy density (i.e., the saturation density) at the neutron star surface as

$$\epsilon_{\rm sat} \sim 8 \times 10^{19} \ \frac{{\rm GeV}}{{\rm cm}^3} \zeta^2 m_{-8}^3 \tilde{B}_0^{9/7} \tilde{\Omega}^{9/7}.$$
 (9)

Pulsar nulling requires efficient axion production,  $\epsilon_0/\epsilon_{\rm br} \propto B^{8/7}\Omega^{9/7} \gtrsim 1$ , and inefficient energy dissipation,  $\epsilon_{\rm br}/\epsilon_{\rm sat} \propto B^{-9/7}\Omega^{5/7} \lesssim 1$ . These conditions can be accommodated for pulsars with large magnetic fields and large periods.

In Fig. 1 we highlight the parameter space for which the axion can dramatically impact the polar cap dynamics. For sufficiently small axion masses (with  $\lambda_a \gg h_{\rm gap}$ ), the axion cloud will uniformly suppress acceleration (and thus pair production and dynamical screening) across the polar cap, leading to a short-lived nulling of the radio signal (see

shaded region in Fig. 1 labeled "Pulsar Nulling"). Since axions are on-shell, any nulling is only temporary, implying the suppression of the radio emission should be approximately periodic with the characteristic timescale set by the axion energy. This implies a well-defined periodic structure in the radio emission on timescales  $t \sim \mathcal{O}(\text{ns} - \mu \text{s})$ , which is observable using current telescopes (see, e.g., [99] for an example of high time-resolution observations).

Incoherent dipole emission—The previous section focused on the case where axions could be treated as being coherently in-phase across the gap, which is only valid for sufficiently light axions. There are two primary differences that arise when one considers the implications of heavier axions (with  $\lambda_a \ll h_{\rm gap}$ ). First, high-mass axions are produced by rapid small-scale fluctuations in the plasma—since the amplitude of these fluctuations is much smaller than the vacuum field, the production rate is suppressed relative to the low-mass limit. Second, the axion field is now incoherent over the gap, meaning one must account for the stochasticity of the axion phase; the incoherence heavily suppresses the effect of the axion on the electrodynamics, and in this regime the existence of local densities  $\epsilon \sim \epsilon_{\rm br}$  may not guarantee the existence of pulsar nulling (see SM where we adopt the approach of Ref. [100]). Nevertheless, the oscillation timescale of the axion field is now sufficiently fast to produce on-shell electromagnetic radiation during the open phase of the gap. In particular, we find that the axion field can produce a narrow, highly beamed, radio line. The origin of this line stems from the fact that an oscillating axion in a background magnetic field behaves equivalently to an oscillating dipole moment. The radiation produced from the oscillating dipole is highly incoherent in the limit  $\lambda_a \gg h_{\rm gap}$ , and is thus heavily suppressed at large masses; nevertheless, the total emission is sufficiently strong to give rise to observable signatures. Assuming that the axion coupling is sufficiently large that the backreaction density is reached, i.e.,  $g_{a\gamma\gamma} \ge g_P^{\min}$  where  $g_P^{\min}$  is the minimum coupling required for pulsar P to produce an axion cloud with density  $\epsilon_{\rm br}$ , and that beaming [101] confines the emission to an angular opening of the size of the polar cap (i.e.,  $\theta_{\rm max} \sim r_{pc}/R_{\rm NS}$ ), we infer (see the SM) an observable flux density of

$$S_{\gamma}(g_{a\gamma\gamma} \ge g_P^{\text{min}}) \equiv \frac{dE_{\gamma}/dt}{d\Omega \mathcal{B} d^2} \sim 38 \text{ Jy} \left(\frac{\xi}{0.1} \frac{2 \text{ kpc}}{d}\right)^2 \frac{\tilde{B}_0^{-2/7} \tilde{\Omega}^{-9/7}}{m_{-6}},$$

where we set the bandwidth to be  $\mathcal{B}=m_a/50$  (note that this includes a suppression from the incoherence). For reasonable parameters this flux can greatly exceed the intrinsic radio flux of the pulsar. Finally, we note that at couplings  $g_{a\gamma\gamma} \leq g_P^{\min}$  the flux density scales as  $S_\gamma \propto g_{a\gamma\gamma}^4$ , and thus this signal is strongest for pulsars reaching the backreaction density.

Results and conclusions—Throughout this Letter we have chosen to use the well-studied Crab pulsar as a reference. There exist pulsars, however, that are more favorable targets to observe both pulsar nulling and nonresonant radio emission. We thus use the Australia Telescope National Facility catalogue to identify better targets for both observables [102-105]. In doing the selection, we enforce that the inferred magnetic field remains below the Schwinger field strength, the pulsar is not a millisecond pulsar, and the spin-down rate is  $\dot{E} > 10^{34}$  erg/s (the latter condition being a rough estimator for when pair cascades are one dimensional [106]). Among the optimal candidates for pulsar nulling is J1119-6127, while the preferred pulsar for radio emission is B1055-52; the parameters for each pulsar are given in Table I of the SM. In the SM we also provide a discussion about pulsar magnetic field evolution [107-111], and identify the parameter space for which backreaction, pulsar nulling, and observable radio emission would arise for each of the three pulsars. These results are combined in Fig. 1 in order to provide an idea of the axion parameter space that could be explored using future observations.

This Letter is an initial investigation into previously unknown phenomena, providing rough estimates illustrating when axion backreaction can occur, and identifying what might be the most robust associated signatures. Figure 1 shows that both pulsar nulling and nonresonant axion-induced radio emission from the polar cap region may provide sensitive probes of axions across a wide range of unexplored parameter space. The complexity of axion electrodynamics in these environments necessitates follow-ups using state-of-the-art numerical simulations (see, e.g., [78,112]) that include strong axion backreaction; this highly nonlinear regime might produce striking new signatures, such as a persistent quasiperiodic suppression of the radio emission and shifts in the neutron star death line.

Acknowledgments—The authors would like to thank Georg Raffelt, Edoardo Vitagliano, Jamie McDonald, Ani Prabhu, Thomas Schwetz, Dion Noordhuis, Andrew Shaw, and Cole Miller for their useful discussions. A. C. acknowledges the hospitality of the Flatiron Center for Computational Astrophysics during the initial stages of this project. S. J. W. acknowledges support from a Royal Society University Research Fellowship (URF-R1-231065), and through the program Ramón y Cajal (RYC2021-030893-I) of the Spanish Ministry of Science and Innovation. This Letter is based upon work from COST Action COSMIC WISPers CA21106, supported by COST (European Cooperation in Science and Technology). This work was supported by a grant from the Simons Foundation (MP-SCMPS-00001470) to A.P. The work of T. J. was supported in part by NSF Grant No. PHY-2309634.

- [1] R. D. Peccei and H. R. Quinn, *CP* conservation in the presence of instantons, Phys. Rev. Lett. **38**, 1440 (1977).
- [2] R. D. Peccei and H. R. Quinn, Constraints imposed by *CP* conservation in the presence of instantons, Phys. Rev. D 16, 1791 (1977).
- [3] S. Weinberg, A new light boson?, Phys. Rev. Lett. **40**, 223 (1978).
- [4] F. Wilczek, Problem of strong *P* and *T* invariance in the presence of instantons, Phys. Rev. Lett. **40**, 279 (1978).
- [5] J. Preskill, M. B. Wise, and F. Wilczek, Cosmology of the invisible axion, Phys. Lett. 120B, 127 (1983).
- [6] M. Dine and W. Fischler, The not so harmless axion, Phys. Lett. **120B**, 137 (1983).
- [7] A. Arvanitaki, S. Dimopoulos, S. Dubovsky, N. Kaloper, and J. March-Russell, String axiverse, Phys. Rev. D 81, 123530 (2010).
- [8] E. Witten, Some properties of O(32) superstrings, Phys. Lett. **149B**, 351 (1984).
- [9] M. Cicoli, M. Goodsell, and A. Ringwald, The type IIB string axiverse and its low-energy phenomenology, J. High Energy Phys. 10 (2012) 146.
- [10] J. P. Conlon, The QCD axion and moduli stabilisation, J. High Energy Phys. 05 (2006) 078.
- [11] P. Svrcek and E. Witten, Axions in string theory, J. High Energy Phys. 06 (2006) 051.
- [12] I. G. Irastorza and J. Redondo, New experimental approaches in the search for axion-like particles, Prog. Part. Nucl. Phys. 102, 89 (2018).
- [13] M. S. Pshirkov and S. B. Popov, Conversion of Dark matter axions to photons in magnetospheres of neutron stars, J. Exp. Theor. Phys. **108**, 384 (2009).
- [14] A. Hook, Y. Kahn, B. R. Safdi, and Z. Sun, Radio signals from axion dark matter conversion in neutron star magnetospheres, Phys. Rev. Lett. 121, 241102 (2018).
- [15] F. P. Huang, K. Kadota, T. Sekiguchi, and H. Tashiro, Radio telescope search for the resonant conversion of cold dark matter axions from the magnetized astrophysical sources, Phys. Rev. D 97, 123001 (2018).
- [16] M. Leroy, M. Chianese, T. D. P. Edwards, and C. Weniger, Radio signal of axion-photon conversion in neutron stars: A ray tracing analysis, Phys. Rev. D 101, 123003 (2020).
- [17] B. R. Safdi, Z. Sun, and A. Y. Chen, Detecting axion dark matter with radio lines from neutron star populations, Phys. Rev. D 99, 123021 (2019).
- [18] R. A. Battye, B. Garbrecht, J. I. McDonald, F. Pace, and S. Srinivasan, Dark matter axion detection in the radio/mm-waveband, Phys. Rev. D **102**, 023504 (2020).
- [19] J. W. Foster *et al.*, Green bank and effelsberg radio telescope searches for axion dark matter conversion in neutron star magnetospheres, Phys. Rev. Lett. **125**, 171301 (2020).
- [20] J. W. Foster, S. J. Witte, M. Lawson, T. Linden, V. Gajjar, C. Weniger, and B. R. Safdi, Extraterrestrial axion search with the breakthrough listen Galactic center survey, Phys. Rev. Lett. 129, 251102 (2022).
- [21] S. J. Witte, D. Noordhuis, T. D. Edwards, and C. Weniger, Axion-photon conversion in neutron star magnetospheres: The role of the plasma in the Goldreich-Julian model, Phys. Rev. D 104, 103030 (2021).

- [22] A. J. Millar, S. Baum, M. Lawson, and M. C. D. Marsh, Axion-photon conversion in strongly magnetised plasmas, J. Cosmol. Astropart. Phys. 11 (2021) 013.
- [23] R. A. Battye, J. Darling, J. McDonald, and S. Srinivasan, Towards robust constraints on axion dark matter using PSR j1745-2900, Phys. Rev. D 105, L021305 (2022).
- [24] S. J. Witte, S. Baum, M. Lawson, M. C. D. Marsh, A. J. Millar, and G. Salinas, Transient radio lines from axion miniclusters and axion stars, Phys. Rev. D 107, 063013 (2023).
- [25] R. A. Battye, M. J. Keith, J. I. McDonald, S. Srinivasan, B. W. Stappers, and P. Weltevrede, Searching for timedependent axion dark matter signals in pulsars, Phys. Rev. D 108, 063001 (2023).
- [26] J. Tjemsland, J. McDonald, and S. J. Witte, Adiabatic axion-photon mixing near neutron stars, Phys. Rev. D 109, 023015 (2024).
- [27] A. Prabhu, Axion production in pulsar magnetosphere gaps, Phys. Rev. D 104, 055038 (2021).
- [28] D. Noordhuis, A. Prabhu, S. J. Witte, A. Y. Chen, F. Cruz, and C. Weniger, Novel constraints on axions produced in pulsar polar cap cascades, Phys. Rev. Lett. 131, 111004 (2023).
- [29] D. Noordhuis, A. Prabhu, C. Weniger, and S. J. Witte, Axion clouds around neutron stars, arXiv:2307.11811.
- [30] A. Iwazaki, Axion stars and fast radio bursts, Phys. Rev. D 91, 023008 (2015).
- [31] Y. Bai and Y. Hamada, Detecting axion stars with radio telescopes, Phys. Lett. B 781, 187 (2018).
- [32] T. Dietrich, F. Day, K. Clough, M. Coughlin, and J. Niemeyer, Neutron star–axion star collisions in the light of multimessenger astronomy, Mon. Not. R. Astron. Soc. **483**, 908 (2019).
- [33] A. Prabhu and N. M. Rapidis, Resonant conversion of dark matter oscillons in pulsar magnetospheres, J. Cosmol. Astropart. Phys. 10 (2020) 054.
- [34] T. D. P. Edwards, B. J. Kavanagh, L. Visinelli, and C. Weniger, Transient radio signatures from neutron star encounters with QCD axion miniclusters, Phys. Rev. Lett. 127, 131103 (2021).
- [35] J. H. Buckley, P. S. B. Dev, F. Ferrer, and F. P. Huang, Fast radio bursts from axion stars moving through pulsar magnetospheres, Phys. Rev. D **103**, 043015 (2021).
- [36] S. Nurmi, E. D. Schiappacasse, and T. T. Yanagida, Radio signatures from encounters between Neutron Stars and QCD-axion minihalos around primordial black holes, J. Cosmol. Astropart. Phys. 09 (2021) 004.
- [37] Y. Bai, X. Du, and Y. Hamada, Diluted axion star collisions with neutron stars, J. Cosmol. Astropart. Phys. 01 (2022) 041.
- [38] A. Prabhu, Axion-mediated transport of fast radio bursts originating in inner magnetospheres of magnetars, Astrophys. J. Lett. **946**, L52 (2023).
- [39] Unit convention:  $c = \hbar = \epsilon_0 = 1$ , and  $e = \sqrt{4\pi\alpha}$ .
- [40] An axion field configuration is a coherent state of many axion particle quanta. Here, we use both field and particle descriptions.
- [41] M. C. Miller *et al.*, PSR J0030 + 0451 mass and radius from *NICER* data and implications for the properties of neutron star matter, Astrophys. J. Lett. **887**, L24 (2019).

- [42] M. C. Miller *et al.*, The radius of PSR J0740 + 6620 from NICER and XMM-Newton data, Astrophys. J. Lett. **918**, L28 (2021).
- [43] D. Wouters and P. Brun, Constraints on axion-like particles from x-ray observations of the hydra galaxy cluster, Astrophys. J. **772**, 44 (2013).
- [44] A. Abramowski *et al.* (H.E.S.S. Collaboration), Constraints on axionlike particles with H.E.S.S. from the irregularity of the PKS 2155-304 energy spectrum, Phys. Rev. D 88, 102003 (2013).
- [45] A. Payez et al., Revisiting the SN1987a gamma-ray limit on ultralight axion-like particles, J. Cosmol. Astropart. Phys. 02 (2015) 006.
- [46] M. Ajello *et al.* (Fermi-LAT Collaboration), Search for spectral irregularities due to photon–axionlike-particle oscillations with the Fermi Large Area Telescope, Phys. Rev. Lett. **116**, 161101 (2016).
- [47] M. Meyer, M. Giannotti, A. Mirizzi, J. Conrad, and M. A. Sánchez-Conde, Fermi Large Area Telescope as a galactic supernovae axionscope, Phys. Rev. Lett. 118, 011103 (2017).
- [48] M. C. D. Marsh, H. R. Russell, A. C. Fabian, B. P. McNamara, P. Nulsen, and C. S. Reynolds, A new bound on axion-like particles, J. Cosmol. Astropart. Phys. 12 (2017) 036.
- [49] C. S. Reynolds, M. C. D. Marsh, H. R. Russell, A. C. Fabian, R. Smith, F. Tombesi, and S. Veilleux, Astrophysical limits on very light axion-like particles from Chandra grating spectroscopy of NGC 1275, Astrophys. J. 890, 59 (2020).
- [50] M. Xiao, K. M. Perez, M. Giannotti, O. Straniero, A. Mirizzi, B. W. Grefenstette, B. M. Roach, and M. Nynka, Constraints on axionlike particles from a hard x-ray observation of betelgeuse, Phys. Rev. Lett. 126, 031101 (2021).
- [51] H.-J. Li, J.-G. Guo, X.-J. Bi, S.-J. Lin, and P.-F. Yin, Limits on axion-like particles from MRK 421 with 4.5-year period observations by ARGO-YBJ and Fermi-LAT, Phys. Rev. D 103, 083003 (2021).
- [52] C. Dessert, J. W. Foster, and B. R. Safdi, X-ray searches for axions from super star clusters, Phys. Rev. Lett. 125, 261102 (2020).
- [53] C. Dessert, A. J. Long, and B. R. Safdi, No evidence for axions from chandra observation of the magnetic white dwarf RE j0317-853, Phys. Rev. Lett. 128, 071102 (2022).
- [54] C. Dessert, D. Dunsky, and B. R. Safdi, Upper limit on the axion-photon coupling from magnetic white dwarf polarization, Phys. Rev. D 105, 103034 (2022).
- [55] V. Anastassopoulos *et al.* (CAST Collaboration), New cast limit on the axion–photon interaction, Nat. Phys. **13**, 584 (2017).
- [56] P. Sikivie, Experimental tests of the "invisible" axion, Phys. Rev. Lett. **51**, 1415 (1983).
- [57] S. DePanfilis, A. Melissinos, B. Moskowitz, J. Rogers, Y. K. Semertzidis, W. Wuensch, H. Halama, A. Prodell, W. Fowler, and F. Nezrick, Limits on the abundance and coupling of cosmic axions at  $4.5 < ma < 5.0 \mu ev$ , Phys. Rev. Lett. **59**, 839 (1987).
- [58] C. Hagmann, P. Sikivie, N. S. Sullivan, and D. B. Tanner, Results from a search for cosmic axions, Phys. Rev. D 42, 1297 (1990).

- [59] C. Hagmann *et al.* (ADMX Collaboration), Results from a high sensitivity search for cosmic axions, Phys. Rev. Lett. 80, 2043 (1998).
- [60] S. J. Asztalos *et al.* (ADMX Collaboration), Large scale microwave cavity search for dark matter axions, Phys. Rev. D 64, 092003 (2001).
- [61] S. J. Asztalos *et al.* (ADMX Collaboration), A SQUID-based microwave cavity search for dark-matter axions, Phys. Rev. Lett. **104**, 041301 (2010).
- [62] N. Du *et al.* (ADMX Collaboration), A search for invisible axion dark matter with the axion dark matter experiment, Phys. Rev. Lett. **120**, 151301 (2018).
- [63] T. Braine et al. (ADMX Collaboration), Extended search for the invisible axion with the axion dark matter experiment, Phys. Rev. Lett. 124, 101303 (2020).
- [64] R. Bradley et al., Microwave cavity searches for darkmatter axions, Rev. Mod. Phys. 75, 777 (2003).
- [65] S. J. Asztalos et al., Improved rf cavity search for halo axions, Phys. Rev. D 69, 011101(R) (2004).
- [66] T. M. Shokair *et al.*, Future directions in the microwave cavity search for dark matter axions, Int. J. Mod. Phys. A 29, 1443004 (2014).
- [67] B. M. Brubaker *et al.* (HAYSTAC Collaboration), First results from a microwave cavity axion search at 24 μeV, Phys. Rev. Lett. 118, 061302 (2017).
- [68] L. Zhong et al. (HAYSTAC Collaboration), Results from phase 1 of the haystac microwave cavity axion experiment, Phys. Rev. D 97, 092001 (2018).
- [69] K. M. Backes *et al.* (HAYSTAC Collaboration), A quantum enhanced search for dark matter axions, Nature (London) 590, 238 (2021).
- [70] B. T. McAllister *et al.*, The organ experiment: An axion haloscope above 15 GHz, 2017.
- [71] N. Crescini et al. (QUAX Collaboration), Axion search with a quantum-limited ferromagnetic haloscope, Phys. Rev. Lett. 124, 171801 (2020).
- [72] J. Choi, S. Ahn, B. R. Ko, S. Lee, and Y. K. Semertzidis, CAPP-8 TB: Axion dark matter search experiment around 6.7 μev, Nucl. Instrum. Methods Phys. Res., Sect. A 1013, 165667 (2021).
- [73] A. A. Melcón *et al.* (CAST Collaboration), First results of the CAST-RADES haloscope search for axions at 34.67 μeV, J. High Energy Phys. 21 (2020) 075.
- [74] F. Wilczek, Two applications of axion electrodynamics, Phys. Rev. Lett. **58**, 1799 (1987).
- [75] M. A. Ruderman and P. G. Sutherland, Theory of pulsars: Polar gaps, sparks, and coherent microwave radiation, Astrophys. J. **196**, 51 (1975).
- [76] A. Timokhin, Time-dependent pair cascades in magnetospheres of neutron stars—I. Dynamics of the polar cap cascade with no particle supply from the neutron star surface, Mon. Not. R. Astron. Soc. 408, 2092 (2010).
- [77] A. N. Timokhin and J. Arons, Current flow and pair creation at low altitude in rotation powered pulsars' force-free magnetospheres: Space-charge limited flow, Mon. Not. R. Astron. Soc. **429**, 20 (2013).
- [78] A. Philippov, A. Timokhin, and A. Spitkovsky, Origin of pulsar radio emission, Phys. Rev. Lett. 124, 245101 (2020).
- [79] P. A. Sturrock, A model of pulsars, Astrophys. J. 164, 529 (1971).

- [80] J. Arons and E. T. Schrlemann, Pair formation above pulsar polar caps: Structure of the low altitude acceleration zone, Astrophys. J. 231, 854 (1979).
- [81] A. N. Timokhin and A. K. Harding, On the polar cap cascade pair multiplicity of Young pulsars, Astrophys. J. **810**, 144 (2015).
- [82] We note that pair production also occurs when  $\alpha < 0$ . These regions correspond to field lines supporting return currents, which serve to carry charges produced at large radii back to the star. For simplicity, we focus here only on the case of  $\alpha > 0$ .
- [83] S. E. Gralla, A. Lupsasca, and A. Philippov, Pulsar magnetospheres: Beyond the flat spacetime dipole, Astrophys. J. 833, 258 (2016).
- [84] S. E. Gralla, A. Lupsasca, and A. Philippov, Inclined pulsar magnetospheres in general relativity: Polar caps for the dipole, quadrudipole and beyond, Astrophys. J. 851, 137 (2017).
- [85] In a fully kinetic calculation, the stop-and-go electron flow configuration leads to an instability and development of a trapped particle population [77]. Future self-consistent simulations will show how the dynamical evolution is modified in the presence of substantial axion background.
- [86] Conversely, if the axion density could remain high enough when a pulsar nears its death, it might prolong the radio emission.
- [87] See Supplemental Material at <a href="http://link.aps.org/supplemental/10.1103/PhysRevLett.133.161001">http://link.aps.org/supplemental/10.1103/PhysRevLett.133.161001</a> for additional details justifying some of the approximations, and outlining the derivations of various quantities quoted in the main text. These include: a look at the velocity distribution of the axion cloud near the neutron star surface, the derivation of the axion-induced electric field, a derivation of the axion production rate, back-reaction density, and energy dissipation rate (both at high and low axion masses), a look at the impact of magneto-rotational spin-down, details on the sensitivity analysis, and a discussion on possible resonant transitions during the phase of pair production.
- [88] A. N. Timokhin and A. K. Harding, On the maximum pair multiplicity of pulsar cascades, Astrophys. J. 871, 12 (2019).
- [89] A. G. Lyne, R. S. Pritchard, and F. Graham Smith, 23 years of Crab pulsar rotational history, Mon. Not. R. Astron. Soc. 265, 1003 (1993).
- [90] A. Lyne, F. Graham-Smith, P. Weltevrede, C. Jordan, B. Stappers, C. Bassa, and M. Kramer, Evolution of the magnetic field structure of the Crab pulsar, Science 342, 598 (2013).
- [91] P. Goldreich and W. H. Julian, Pulsar electrodynamics, Astrophys. J. 157, 869 (1969).
- [92] A. K. Harding and A. G. Muslimov, Particle acceleration zones above pulsar polar caps: Electron and positron pair formation fronts, Astrophys. J. 508, 328 (1998).
- [93] There we make use of Refs. [94–97] to perform our computations.
- [94] G. G. Raffelt, Stars as Laboratories for Fundamental Physics (University of Chicago Press, Chicago, 1996).
- [95] M. Beutter, A. Pargner, T. Schwetz, and E. Todarello, Axion-electrodynamics: A quantum field calculation, J. Cosmol. Astropart. Phys. 02 (2019) 026.

- [96] J. D. Jackson, Classical Electrodynamics (Wiley, New York, 1998).
- [97] A. Caputo, S. J. Witte, D. Blas, and P. Pani, Electromagnetic signatures of dark photon superradiance, Phys. Rev. D 104, 043006 (2021).
- [98] J. Arons and J. J. Barnard, Wave propagation in pulsar magnetospheres-Dispersion relations and normal modes of plasmas in superstrong magnetic fields, Astrophys. J. 302, 120 (1986).
- [99] T. Hankins, J. Kern, J. Weatherall, and J. Eilek, Nanosecond radio bursts from strong plasma turbulence in the Crab pulsar, Nature (London) 422, 141 (2003).
- [100] E. A. Tolman, A. A. Philippov, and A. N. Timokhin, Electric field screening in pair discharges and generation of pulsar radio emission, Astrophys. J. Lett. 933, L37 (2022).
- [101] Beaming is a consequence of the dense plasma layers surround the boundary of the polar cap, which serve as mirrors, confining the radiation (see SM).
- [102] F. Jankowski, M. Bailes, W. van Straten, E. Keane, C. Flynn, E. Barr, T. Bateman, S. Bhandari, M. Caleb, D. Campbell-Wilson *et al.*, The utmost pulsar timing programme I: Overview and first results, Mon. Not. R. Astron. Soc. **484**, 3691 (2019).
- [103] M. Bell, T. Murphy, S. Johnston, D. Kaplan, S. Croft, P. Hancock, J. Callingham, A. Zic, D. Dobie, J. Swiggum et al., Time-domain and spectral properties of pulsars at 154 MHz, Mon. Not. R. Astron. Soc. 461, 908 (2016).
- [104] F. Jankowski, W. Van Straten, E. Keane, M. Bailes, E. Barr, S. Johnston, and M. Kerr, Spectral properties of 441 radio pulsars, Mon. Not. R. Astron. Soc. 473, 4436 (2018).
- [105] P. Weltevrede, S. Johnston, and C. M. Espinoza, The glitch-induced identity changes of PSR j1119- 6127, Mon. Not. R. Astron. Soc. 411, 1917 (2011).
- [106] A. Philippov and M. Kramer, Pulsar magnetospheres and their radiation, Annu. Rev. Astron. Astrophys. 60, 495 (2022).
- [107] A. Spitkovsky, Time-dependent force-free pulsar magnetospheres: Axisymmetric and oblique rotators, Astrophys. J. 648, L51 (2006).
- [108] A. Philippov, A. Tchekhovskoy, and J.G. Li, Time evolution of pulsar obliquity angle from 3d simulations of magnetospheres, Mon. Not. R. Astron. Soc. 441, 1879 (2014).
- [109] A. Lyne, F. Graham-Smith, P. Weltevrede, C. Jordan, B. Stappers, C. Bassa, and M. Kramer, Evolution of the magnetic field structure of the Crab pulsar, Science 342, 598 (2013).
- [110] A. Lyne, C. Jordan, F. Graham-Smith, C. Espinoza, B. Stappers, and P. Weltevrede, 45 years of rotation of the Crab pulsar, Mon. Not. R. Astron. Soc. **446**, 857 (2015).
- [111] S. Rookyard, P. Weltevrede, and S. Johnston, Constraints on viewing geometries from radio observations of  $\gamma$ -ray-loud pulsars using a novel method, Mon. Not. R. Astron. Soc. **446**, 3367 (2015).
- [112] F. Cruz, T. Grismayer, A. Y. Chen, A. Spitkovsky, and L. O. Silva, Coherent emission from QED cascades in pulsar polar caps, Astrophys. J. Lett. **919**, L4 (2021).